IMAGING OF COMMON MALIGNANT ABDOMINAL TUMORS IN CHILDREN

NATHAN DAVID P. CONCEPCION, MD, MIRIAM C. DE LEON, MD, AND BERNARD F. LAYA, MD, DO

ABSTRACT

Abdominal masses in children are diverse in etiology and origin. They comprise various organ systems such as the gastrointestinal, genitourinary, and endocrine system among others. The patient's age is very important in differentiating the potential cause of abdominal masses. In neonates, most abdominal masses are benign. The incidence of malignancy increases in older children and adolescents. Patients with underlying abdominal malignancy present with constitutional symptoms such as fever, weight loss, and a palpable abdominal mass, but some present with nonspecific signs especially in the early stage of disease. An organized approach to the diagnosis of abdominal malignancies includes accurate localization and characterization of the tumor. Medical imaging plays a very crucial role in the initial assessment, localization, diagnosis, and follow-up of these neoplasms.

This article aims to provide an overview of the common primary malignant abdominal tumors in children encountered at St. Luke's Medical Center. It discusses the value of the different imaging modalities and emphasizes the typical imaging characteristics of these tumors. The epidemiology of these tumors are also presented.

Authors' Affiliation: Drs. Concepcion and Laya, Institute of Radiology, St. Luke's Medical Center, 279 E. Rodriguez Sr. Blvd, Quezon City, 1112, Philippines and 32nd Street, Bonifacio Global City, Taguig City 1634, Philippines. Dr. De Leon, Institute of Radiology, St. Luke's Medical Center, 32nd Street, Bonifacio Global City, Taguig City 1634, Philippines.

Correspondence and reprints: Dr. Nathan David P. Concepcion, Institute of Radiology, St. Luke's Medical Center, 32nd Street, Bonifacio Global City, Taguig City 1634, Philippines

E-mail: nathanmd_prg@yahoo.com

Neoplastic abdominal malignancies, particularly those originating from embryonal tissue (such as hepatoblastoma and nephroblastoma) and neural crest cells (such as neuroblastoma), are often seen in children. Neoplasms commonly seen in adults such as carcinoma involving various visceral organs, although less frequent, are also seen in the pediatric age group.Although histopathological confirmation remains the gold standard for diagnosis, some of these abdominal malignancies have characteristic imaging appearances that aid in accurate diagnosis even prior to biopsy. In most cases, medical imaging helps localize and characterize the abnormality, which along with clinical and laboratory clues, help in the diagnosis, staging, treatment, post-therapeutic management, and assessment of sequelae.

A plain radiograph although often obtained has very limited value and may only show non-specific findings. Ultrasound (US) therefore is the primary screening tool for patients suspected to have an abdominal mass. Sometimes, the abdominal mass is detected as an incidental finding when the child is referred for other clinical problems. Cross-sectional imaging, i.e. Computed Tomography (CT) or Magnetic Resonance Imaging (MRI), is done for the diagnosis, staging, pre-operative management, follow-up, and monitoring. CT is fast and more readily accessible, with superb anatomical delineation. However, it is important to make sure that each CT scan performed is clinically justified and that conscious efforts to reduce unnecessary high dose radiation exposure shall be done according to principle of ALARA (as low as reasonably achievable).

The typical radiographic features of the tumors included in this article will aid the radiologists, radiologists-in-training or even the clinicians to suggest or confirm a diagnosis with confidence while waiting for the histopathology results.

SPECIFIC ABDOMINAL TUMORS

HEPATOBLASTOMA

Epidemiology

Hepatoblastoma is the most common primary liver malignancy in childhood and about 90% develops during the first 5 years of life. The peak incidence is at 1-2 years of age with 2:1 male to female ratio. It usually presents as a palpable mass in the right upper quadrant with nonspecific symptoms including pain, weight loss, irritability,

vomiting, jaundice, and even precocious puberty caused by secretion of chorionic gonadotropins and testosterone by tumor hepatoblasts. Alphafetoprotein (AFP) is markedly elevated in 90% of patients. It can also be used to monitor response to therapy and detect tumor recurrence.

Association with Beckwith-Wiedemann Syndrome (macroglossia, macrosomia, midline abdominal wall defects, neonatal hypoglycemia, ear creases or pits), familial adenomatous polyposis, type IA glycogen storage disease, fetal alcohol syndrome, Wilms' tumor and trisomy[18] has been discussed in literature.[1]

Imaging

The imaging characteristics of hepatoblastomas are reflective of its histologic composition. There are two broad histologic types, namely epithelial and mixed epithelial-mesenchymal types. The epithelial hepatoblastomas appear homogeneous while the mixed type is heterogeneous due to osteoid, cartilaginous and fibrous components. The tumor is generally well-circumscribed with lobulated contour.

Plain radiographs may show hepatomegaly, a right upper quadrant mass, calcifications, or mass effect to adjacent organs (Figure 1A).

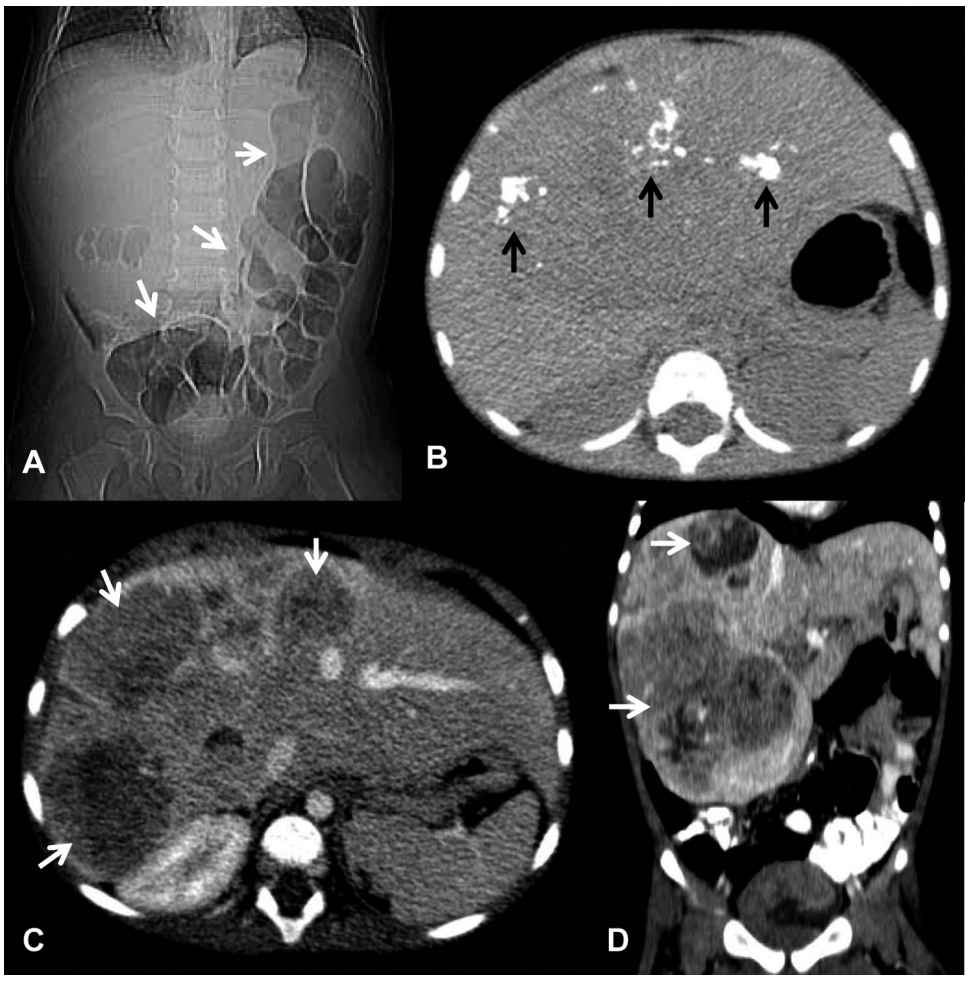

Figure 1. A 23-month-old girl with a hepatoblastoma

1A. CT surview showing a right upper quadrant mass displacing the bowels (*white arrows*) inferiorly and to the left

1B. Non-contrast axial CT image demonstrating coarse calcifications (*black arrows*) in the liver

1C-D. Heterogeneous lobulated mass (*white arrows*) as seen on the post-contrast axial (C) and coronal reformatted (D) CT images; Enhancement is mild and lesser than the normal liver.

US should be the initial screening modality. Hepatoblastomas appear hyperechoic relative to the adjacent normal liver. It may contain septation, calcification and areas of hemorrhage or necrosis. Color Doppler imaging can assess the hepatic or portal veins for vascular invasion with thrombus formation. Presence of flow within the thrombus is an important feature to differentiate neoplastic from non-neoplastic thrombus.

On CT, hepatoblastomas show decreased attenuation relative to normal parenchyma. It may be solitary or multifocal. Calcifications are usually coarse and chunky, stippled or amorphous. Enhancement is mild and less when compared to the liver (Figures 1B-D). Arterial phase may show mild peripheral and septal enhancement. Delayed images show a relative isodense or hypodense mass. CT angiography may detect vascular invasion and assess resectability.

MRI demonstrates a tumor that is hypointense on T1-weighted (T1W) images and hyperintense on the T2-weighted (T2W) images relative to the normal parenchyma. Septations and hemorrhages may be expected. Calcifications may be also seen but are best demonstrated in CT. Vascular invasion is best appreciated in the gradient-echo sequence. MR angiography may also be useful prior to resection.[1]

The most common site of metastasis is the lungs, followed by lymph nodes, bone, brain, eye and ovary.[1,2]

WILMS' TUMOR / NEPHROBLASTOMA

Epidemiology

Nephrogenic rests are embryonal renal parenchyma that persists in infancy. These are present in less than 1% of infants and may undergo malignant transformation into a nephroblastoma, more commonly known as Wilms' tumor, named after the German surgeon Max Wilms who described it in 1899. The cause of malignant transformation is unknown.[3]

Wilms' tumor is the most common abdominal malignancy and most common primary renal malignancy in children, accounting for 87% of renal masses. Age of presentation is from 1-11 years with peak age at about 3.5 years. It can be bilateral in 10% of cases and occurs almost exclusively in patients with nephroblastomatosis.[4] It is slightly more common in girls.[5]

Wilms' tumor may be part of a syndrome, typically occuring between 2 and 24 months. WT1 and WT2 genes on chromosome 11 have been implicated. WT1 gene is associated with WAGR syndrome (**W**ilms' tumor, **A**niridia, **G**enitourinary abnormalities, mental **R**etardation) or Drash syndrome (Wilms' tumor, male pseudohermaphroditism, progressive glomerulonephritis). WT2 gene is associated with Beckwith-Wiedemann syndrome or hemihypertrophy.[6]

Clinically, Wilms' tumor presents as a palpable, frequently painless abdominal mass. Hematuria may be present and hypertension may be due to renin production by the tumor.

Imaging

Plain radiographs could show a flank mass obliterating the psoas shadow. There may be displacement of adjacent structures particularly the bowel loops. Calcifications are seen in 9-20% (Figure 2A).[3,5]

US shows a heterogeneous mass with hypoechoic (necrosis, hemorrhage or cysts) and/or hyperehoic areas (calcification or fat).[3,5,6] Color Doppler examination of the inferior vena cava and renal veins may detect thrombus formation.

CT is the preferred imaging modality for tumor characterization and extent, as well as for regional, vascular and lymph node invasion. It demonstrates a heterogeneous mass due to calcification, fat, hemorrhage, necrosis and/or cysts. The normal renal parenchyma surrounding the mass on either side forms sharp angles ("beak" or "claw" sign). Enhancement is less than the adjacent renal parenchyma (Figures 2B-C). Intravenous contrast is mandatory to detect tumor invasion into the inferior vena cava and/or renal veins (Figures 3A-B), synchronous tumors and associated nephrogenic rests.[6] Vessel invasion is a distinguishing feature of Wilms' tumor compared to neuroblastoma which usually encases adjacent vessels.

On MRI, Wilms' tumor is hypointense on T1W and hyperintense on T2W sequences, and enhances heterogeneously after gadolinium administration. MRI is still the most sensitive modality to assess caval patency.[6] Common sites for metastases are the lung (85%), liver, bone and brain.[6]

NEUROBLASTOMA

Epidemiology

Neuroblastoma, described by German physician Rudolf Virchow in 1863, is the second most common abdominal tumor in children following Wilms' tumor. It is the most common adrenal tumor of infancy and childhood, and also ranks third most common pediatric malignancy after leukemia and CNS tumors.[7]

The incidence in children younger than 15 years is 10.5 per 1 million per year (8-10% of childhood solid tumors). The peak age is less than 4 years, with a median of 23 months. More than 90% occur in patients younger than 10 years.[5]

Imaging

Neuroblastoma usually presents as a large, heterogeneous, poorly marginated, suprarenal mass. Calcifications

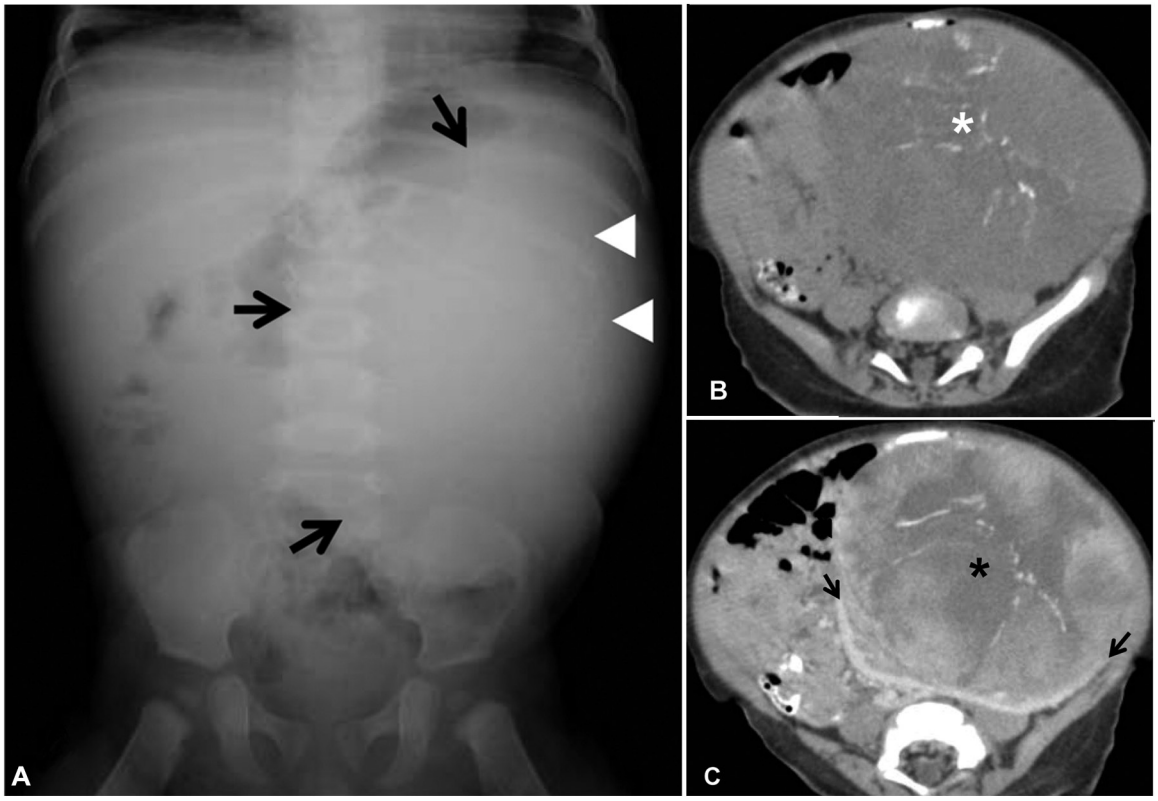

Figure 2. Wilms' tumor in a 7-month-old boy

2A. Abdominal radiograph in an AP supine view showing a soft tissue mass (*black arrows*) with calcifications (*white arrowheads*) in the left hemiabdomen causing displacement of the stomach and bowel loops

2B-C. Non-contrast (B) and contrast-enhanced (C) axial CT images demonstrating a heterogeneous enhancing mass with stippled calcifications (*white asterisk*); Enhancement is lesser than the normal renal cortex (*black asterisk*). "Claw sign" (*black arrows pointing to the normal renal edges*) may also be seen.

are seen on radiographs (30%) and on CT (85%), more common than in Wilms' tumor. This tumor has a tendency to displace the kidney inferiorly, and cross the midline with encasement of the adjacent arteries such as the celiac axis and superior mesenteric artery (Figures 4A-B).

MRI is more sensitive than CT due to its higher soft tissue contrast resolution that allows excellent tumor origin detection. Neuroblastomas are heterogeneous and low in signal on T1W and bright on T2W images. Calcifications are present in 80-90% but are better seen on CT. Areas of hemorrhage are bright on T1W images and cystic changes have high signal on T2W images.[8]

The imaging modality of choice in localizing the tumor, assessing metastasis and staging of disease is meta-iodobenzylguanidine (MIBG) scintigraphy (88-93% sensitive, 83-92% specific).[6]

Metastasis is most frequently encountered in the bone and liver.[9] Periorbital ecchymosis ("raccoon eye") is seen in 5.4% of cases.[10,11] In 10-43%, opsoclonus, Horner syndrome, ocular motility defects and/or blindness may also be observed.[11]

PANCREATOBLASTOMA

Epidemiology

Pediatric pancreatic tumors in general are rare but pancreatoblastoma, also known as infantile cancer of the pancreas[12], is the most common primary malignancy of the pancreas in children. It occurs more commonly in East Asians, with the mean presentation age of 4-5 years.[13,14] There is slight male predilection.

Alphafetoprotein (AFP) levels are elevated in 25-55% and thus may be used for diagnosis and follow-up. The tumor may also secrete adrenocorticotropic hormone (ACTH).[14]

These tumors have been linked with Beckwith-Wiedemann syndrome.[14,15]

Imaging

Pancreatoblastoma has an insidious course and the tumor tends to be large, approximately 5-10 cm.[12] This tumor may be multi-lobulated, well-circumscribed and

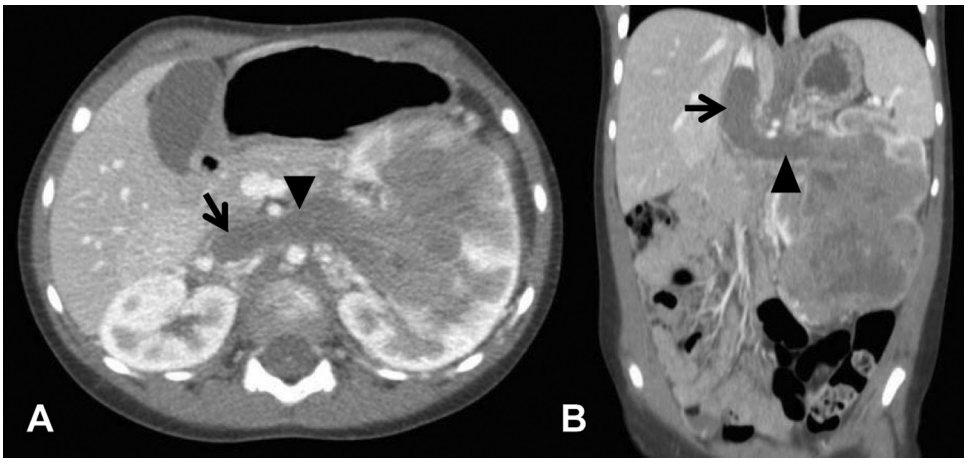

Figure 3. A 6-year-old girl with a Wilms' tumor

3A-B. Wilms' tumor in a 6-year-old girl shown in axial (A) and coronal reformatted (B) CT images having tumor invasion with thrombus formation in the left renal vein (*arrow head*) up to the inferior vena cava (*arrow*)

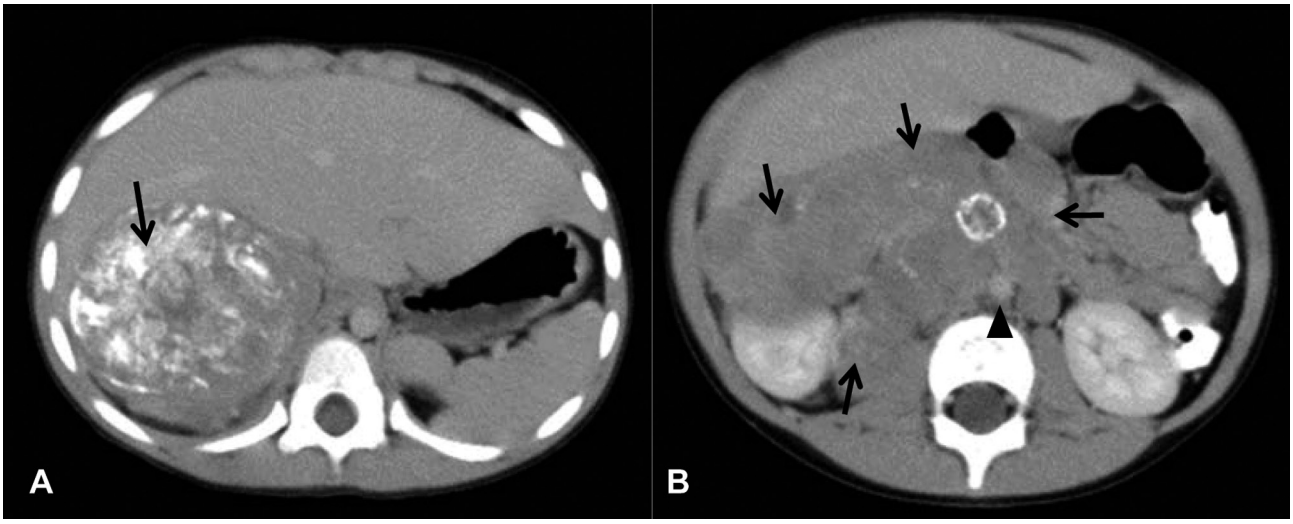

Figure 4. A 2-year-old male diagnosed to have neuroblastoma

4A. Axial non-contrast CT image shows a calcified soft tissue mass (*arrow*) posterior to the liver

4B. Axial post-contrast CT image demonstrates a lobulated mass (*arrows*) crossing the midline encasing the aorta (*arrowhead*)

exophytic.[12,14,16] It arises more commonly from the body or tail.[17]

US usually demonstrate a well demarcated, heterogeneous but predominantly hypoechoic mass with areas of necrosis or cysts (Figure 5A). Color Doppler study may show mild tumor and/or rim vascularity. It may contain stippled calcification and could also encase vessels, similar to neuroblastoma.[14,17]

On CT, the tumor appears as a large, heterogeneous solitary mass with a lower attenuation than the liver.[17] Peripheral calcification may be seen. There is mild heterogeneous enhancement and a well-defined, enhancing rim.[18]

MRI provides increased sensitivity in revealing tumor spread to the liver. Even on a non-contrast study, vascular invasion by a tumor thrombus may be shown.[19] Pancreatoblastomas have low to intermediate T1W and high T2W signal. On dynamic contrast study, the rim will show rapid arterial enhancement with late washout, representing its vascular nature. Non-enhancing T2 bright signals represent areas of necrosis (Figures 5B-F).[13,16,20] Diffusion-weighted images demonstrate marked restricted diffusion (*b* value of 500 sec/mm^2 and low ADC value) due to its increased or dense cellularity.[16]

Pancreatoblastomas are also often difficult to distinguish from other childhood abdominal masses such as hepatoblastoma, Wilms' tumor, neuroblastoma or lymphoma.[15]

Pinpointing the organ of origin would be challenging when the mass is large. Although primary pancreatic neoplasms are rare in childhood, it should be included in the differential diagnosis of tumors arising in or near the lesser sac[21]or in the mesentery.[12,18]

LYMPHOMA

Epidemiology

Hodgkin's disease (HD) and non-Hodgkin's lymphomas (NHL) constitute 10-15% of all childhood cancers in developed countries and are third in frequency after acute leukemias and brain tumors.[22]

The prevalence of HD in developing countries peaks before adolescence. HD is very rare in children younger than 5 years. The prevalence in males and females is similar.[22]

For NHL, the prevalence is much higher in developing countries. Unlike in HD, the prevalence of NHL increases steadily with age.[22] According to Globocan in 2012, the estimated incidence rate of NHL in the Philippines for patients 0-14 years of age is 0.4 with an age-standardized rate

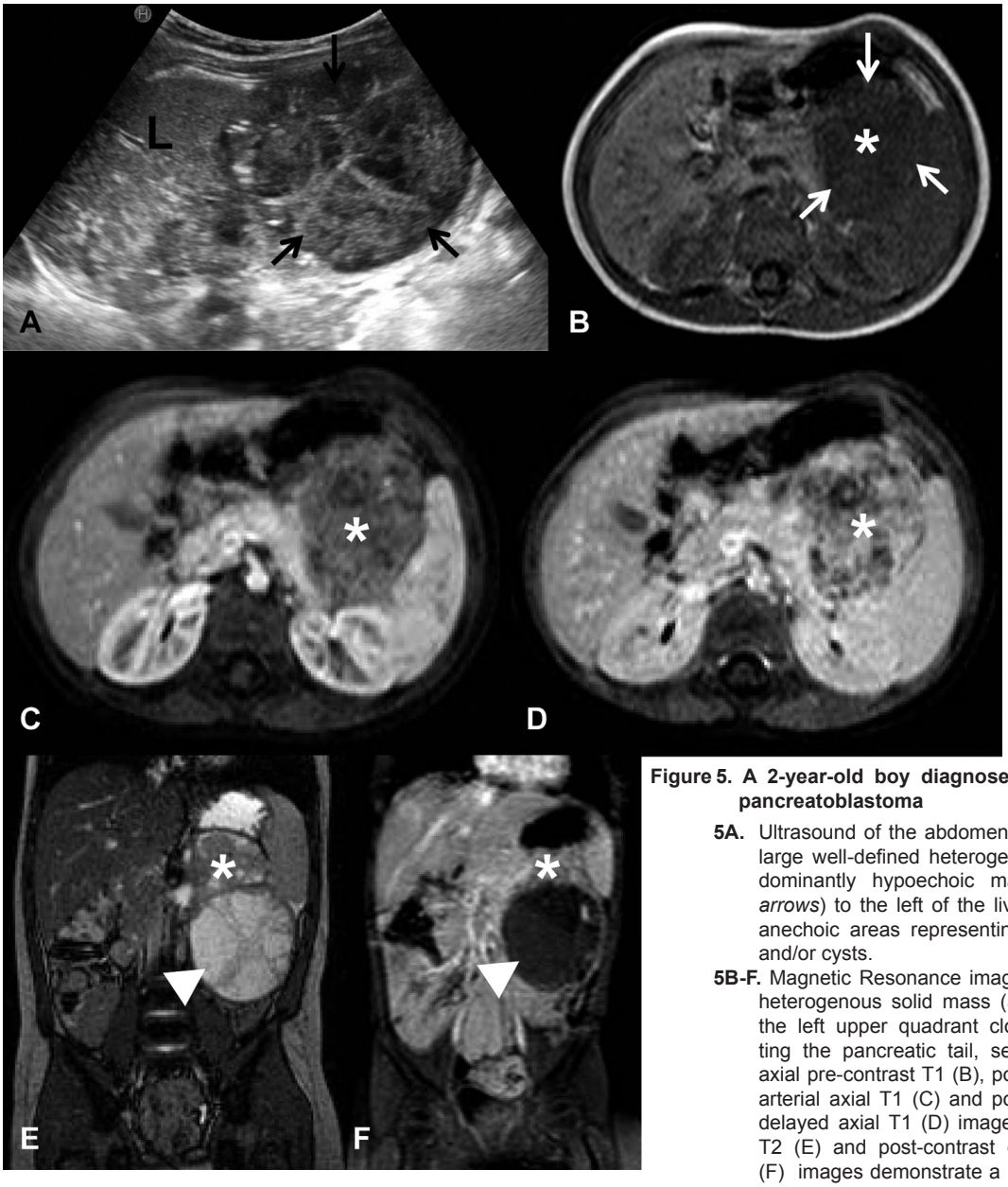

Figure 5. A 2-year-old boy diagnosed to have pancreatoblastoma

5A. Ultrasound of the abdomen displays a large well-defined heterogeneous predominantly hypoechoic mass (*black arrows*) to the left of the liver (L) with anechoic areas representing necrosis and/or cysts.

5B-F. Magnetic Resonance images show a heterogenous solid mass (*asterisk*) in the left upper quadrant closely abutting the pancreatic tail, seen on the axial pre-contrast T1 (B), post-contrast arterial axial T1 (C) and post-contrast delayed axial T1 (D) images. Coronal T2 (E) and post-contrast coronal T1 (F) images demonstrate a large multiseptated cystic / necrotic component (*arrowheads*) inferior to the above-mentioned solid mass.

of 3.1 per 100,000. It is slightly more common in males.[23]

Lymphoma may involve the central nervous system, head and neck, thorax, gonads, and bone at some stage of the disease, but this article only reviews its intra-abdominal involvement.

Imaging

Histologic analysis is necessary for a definitive diagnosis of lymphoma. Nodular sclerosis is the most common subtype of HD while the most common subtype of NHL involving the abdomen are Burkitt's lymphoma and large B-cell lymphomas.[22]

Nodal and splenic involvement is more common in Hodgkin's disease at onset, whereas for non-Hodgkin's lymphomas, extranodal involvement is more frequent. Primary disease in HD appearing in a subdiaphragmatic site is rare (about 3%). In NHL, the most frequently involved sites are intra-abdominal and intrathoracic.[22]

US and CT are the main modalities in patients with abdominal lymphoma. MRI is used mainly when neurologic symptoms emerge.[22]

Positron emission tomography (PET) combined with CT (PET-CT) after treatment is useful in evaluating residual masses. The absence of uptake is a reliable predictor of remission in HD, and increased uptake is associated with residual disease and progression.[24] In NHL, the routine use of PET is unnecessary for staging, although it may be useful to assess the response to therapy.[22]

Various systems and abdominal organs may be affected by lymphoma, and the characteristic findings seen in these areas are discussed in the next sections.

A. Gastrointestinal Tract

The gastrointestinal tract, particularly the distal ileum, cecum, ascending colon and appendix, is the most common site for NHL. The tumor is usually circumferential, progressively infiltrating the bowel wall. Multifocal involvement is not uncommon.

With US, there is a significant hypoechoic bowel wall thickening with loss of stratification. Bowel wall thickening is also observed in Crohn's disease (CD), but the loss of stratification in CD is usually a late finding and the wall thickening is lesser than in lymphoma. A hypoechoic or complex mass with necrotic areas may likewise be detected in lymphoma.

CT commonly shows marked bowel wall thickening, either focal or diffuse, with soft-tissue attenuation and minimal enhancement. The lumen may be stenotic in both lymphoma and CD, but lymphoma may also show luminal dilatation due to replacement of the muscular layers by the tumor.[22]

B. Mesenteric and Retroperitoneal Lymph Nodes

Nodal involvement can be seen in HD, and also in NHL when associated with primaries in the small bowel. There may be a loss of nodal definition within a confluent mass. A central mass may also be found in the mesenteric and retroperitoneal regions along the great vessels (Figures 6A-B). Bilateral prevertebral masses may also be seen, which may subsequently form a single confluent mass.

Encasement of abdominal structures is common, leading to impairment of venous circulation in the lower limbs when the aorta and inferior vena cava are involved, or to obstructive uropathy when the ureters are encased. A "sandwich sign" is produced with encasement of the root of the mesentery and superior mesenteric artery (Figure 7).[22]

C. Kidney

Primary renal lymphoma is about 3% in patients of all ages and is usually seen in terminal phases of NHL. Burkitt's lymphoma has the highest frequency of renal infiltration. Three patterns of infiltration are known: bilateral multiple small nodules (60-70%), solitary mass (10-20%), and diffuse infiltration (5-10%). Hematogenous dissemination is the most common source, although infiltration from adjacent lymph nodes is also common. Renal disease in HD is very rare.

Renal lymphomas appear homogeneous and hypoechoic or anechoic on US. Anechoic lesions may mimic cysts, but the absence of backwall enhancement suggests that the mass is solid. On CT, lymphomatous masses have relatively low attenuation and show minimal enhancement (Figure 8A-B). Focal necrosis or hemorrhage may be seen in larger lesions.[22]

D. Spleen

Involvement of the spleen for all ages is more common in HD (35%) compared to NHL (15%). The spleen can be diffusely infiltrated resulting in homogeneous splenomegaly or can have solitary or multiple nodules. These nodules are hypoechoic relative to the normal spleen on US and are non-enhancing, low attenuation masses on CT (Figure 8C). MRI may show a spotted appearance on T2W images caused by fibrosis, hemorrhage, edema or necrosis. Calcifications could be seen. Splenomegaly may be mild to moderate but without lymphomatous infiltration.[22]

E. Pancreas

Pancreatic infiltration is unusual. It may occur with widely disseminated pre-terminal disease. Diffuse enlargement of the entire gland could be seen or may appear as focal hypoechoic or hypodense areas on US and CT (Figure 8C-D), respectively. Occasionally, peripancreatic

Figure 6. An 18-year-old male with Hodgkin's disease

6A. Contrast-enhanced axial CT image showing encasement of the aorta (*A*) by the nodal masses (*arrows*) with displacement and slight compression of the inferior vena cava (*IVC*)

6B. Coronal reformatted CT image demonstrates the enlarged nodes (*arrows*) along the aorta (*A*), renal arteries and inferior vena cava (*IVC*)

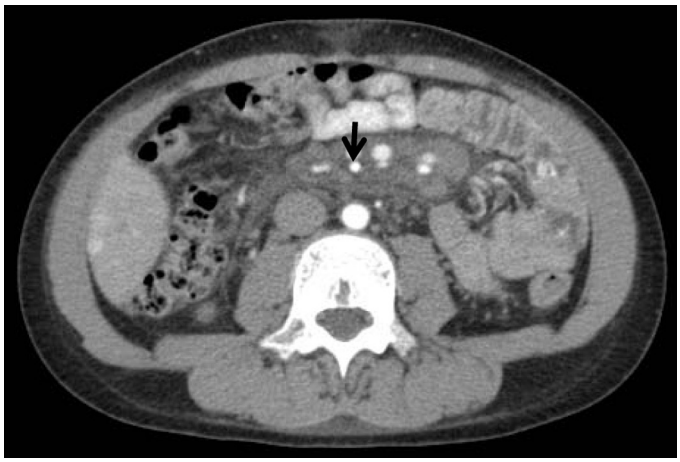

Figure 7. A 14-year-old male with nodal disease encasing the superior mesenteric artery (*arrow*), "*sandwich sign*"

retroperitoneal lymph nodes may enlarge and invade or distort the pancreas.[22]

F. Liver

The liver is rarely involved without associated involvement of the spleen. It is more common in NHL than in HD, and usually in the form of diffuse infiltration, although nodular disease has also been observed (Figure 8E). Patients may have hepatomegaly but with no histologic evidence of lymphoma (about 50%), and patients with normal-sized livers can have extensive lymphomatous infiltration. US and CT findings are similar to those in the spleen.[22]

G. Peritoneum and Omentum

Peritoneal and omental involvement are not common. If detected, extensive bowel or mesenteric infiltration is also seen, or the disease is already disseminated. On US, the areas of involvement are relatively hypoechoic; while on CT, "omental cakes" are observed between the bowel and the abdominal wall. Ascites is also frequent.[22]

RHABDOMYSARCOMA (URINARY BLADDER)

Epidemiology

Rhabdomyosarcoma (RMS) is the most common type of soft tissue sarcoma among children.[8,25,26,27] Embryonal and alveolar RMS are the two main histological subtypes,

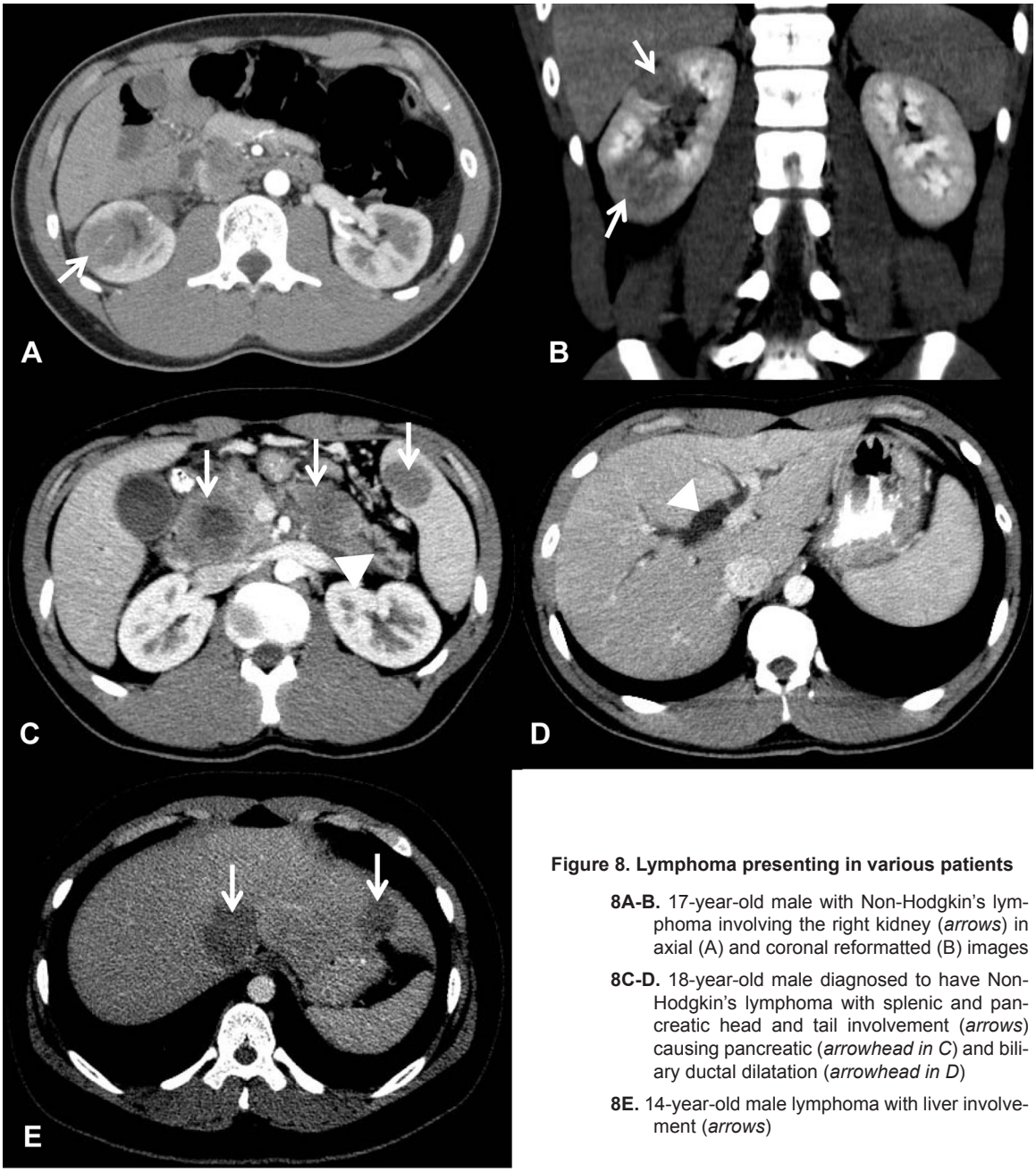

Figure 8. Lymphoma presenting in various patients

8A-B. 17-year-old male with Non-Hodgkin's lymphoma involving the right kidney (*arrows*) in axial (A) and coronal reformatted (B) images

8C-D. 18-year-old male diagnosed to have Non-Hodgkin's lymphoma with splenic and pancreatic head and tail involvement (*arrows*) causing pancreatic (*arrowhead in C*) and biliary ductal dilatation (*arrowhead in D*)

8E. 14-year-old male lymphoma with liver involvement (*arrows*)

where the embryonal type (61%) is more common[8,25,26] and has the better prognosis.[25] These two subtypes account for over 90% of cases in children less than 5 years. It is slightly more common in males.[8,26] The age-standardized annual incidence rate is 4-7 per million.[25,27]

These tumors are highly malignant neoplasms coming from existing skeletal muscle or from the pluripotential mesenchymal cells of connective tissue.[27] This tumor arises in the genitourinary system in 20-34% of cases.[8,25,27,28] Children with genitourinary RMS may present with urinary retention, irritative voiding, hematuria, bladder outlet obstruction, incontinence or urinary infection.[8,25]

Imaging

Rhabdomyosarcomas appear as a solid, lobulated, soft tissue mass with well-defined margins.

Conventional radiography has a limited use. If intra-

venous pyelography or cystography is performed, RMS will appear as a filling defect within the bladder and may show ureteral obstruction.

US is often the first imaging modality used and is also good for follow-up. RMS is a well-defined, heterogeneous mass (Figure 9A) that can show significantly increased flow.[25,28] The intravesical mass and bladder wall involvement may be seen. Ascites, hydroureter or hydronephrosis from obstruction may also be observed.[8]

CT may likewise demonstrate a lobulated heterogeneously enhancing mass and it will better delineate extravesical extension, as well as nodal[28] and solid organ metastases.

MRI is the primary imaging modality. However, the imaging characteristics are nonspecific. Like most soft-tissue tumors, the tumors have intermediate signal on T1W and intermediate to high signal on T2W images. RMS in general shows strong enhancement (Figures 9B-D). Tumors may be lobulated and septated, and rarely may show a cystic appearance. Vascular encasement can be observed.[25]

Metastasis from rhabdomyosarcoma is to the lung (36%), bone marrow (22%), and bone (7%).[8]

Germ cell tumor of the ovary

Epidemiology

Malignant ovarian neoplasms are uncommon and account for less than 2% of all pediatric cancers.[30,31] Incidence of malignant ovarian tumors is 0.102 per 100,000 per year in girls age 9 years or younger, with a 10-fold increase in girls age 10-19 years, to 1,072 per 100,000 per year. It is uncommon for infants younger than 1 year to have a malignant ovarian neoplasm.[30]

Germ cell tumors are the most common ovarian neoplasms (68-80%) in children and adolescents.[29,30] The most common histological subtype is the malignant teratoma (38.5%), and dysgerminoma (33%).[30]

Figure 9. A 14-month-old boy with Urinary Bladder (UB) rhabdomyosarcoma

9A. Ultrasound of the urinary bladder shows a lobulated heterogeneous mass (*arrow*) at the floor with a large extravesical component (*asterisk*).

9B-D. Magnetic Resonance images of the same patient again demonstrates the lobulated UB floor mass (*arrows*) on axial pre-contrast T1 in phase (B) as well as the strongly enhancing mass (*arrows*) with extravesical component (*asterisks*)compressing on the rectum on sagittal T2 (C) and post-contrast sagittal T1 (D) images.

The most common presenting symptom for germ cell tumors is abdominal pain, followed by abdominal distention and a palpable mass.

Mature cystic teratoma is the most common type of ovarian neoplasm in children and the only benign form.

Immature teratoma however, has a worse prognosis and typically affect a younger age group.This tumor usually demonstrates prominent areas of soft tissue, scattered foci of fat and fewer calcifications. The more solid component favors the immature types (Figures 10 A-C). Bilateral involvement does not necessarily infer a malignant process. Increased serum levels of beta human chorionic gonadotrophin (β-HCG) and alpha fetoprotein (AFP) are virtually diagnostic for malignant ovarian germ cell tumors when positive, although they might be positive in only 50% of the cases. These markers may also be used for relapse surveillance.

Dysgerminoma is the least differentiated type of germ cell tumors and is the most common form of malignant ovarian neoplasm mainly affecting adolescents and young girls. Lactate dehydrogenase (LDH) levels are elevated with these tumors. The tumor appears as a solid, lobulated mass with thin fibrovascular septa that typically enhance after contrast infusion. It is not uncommon to observe cal-

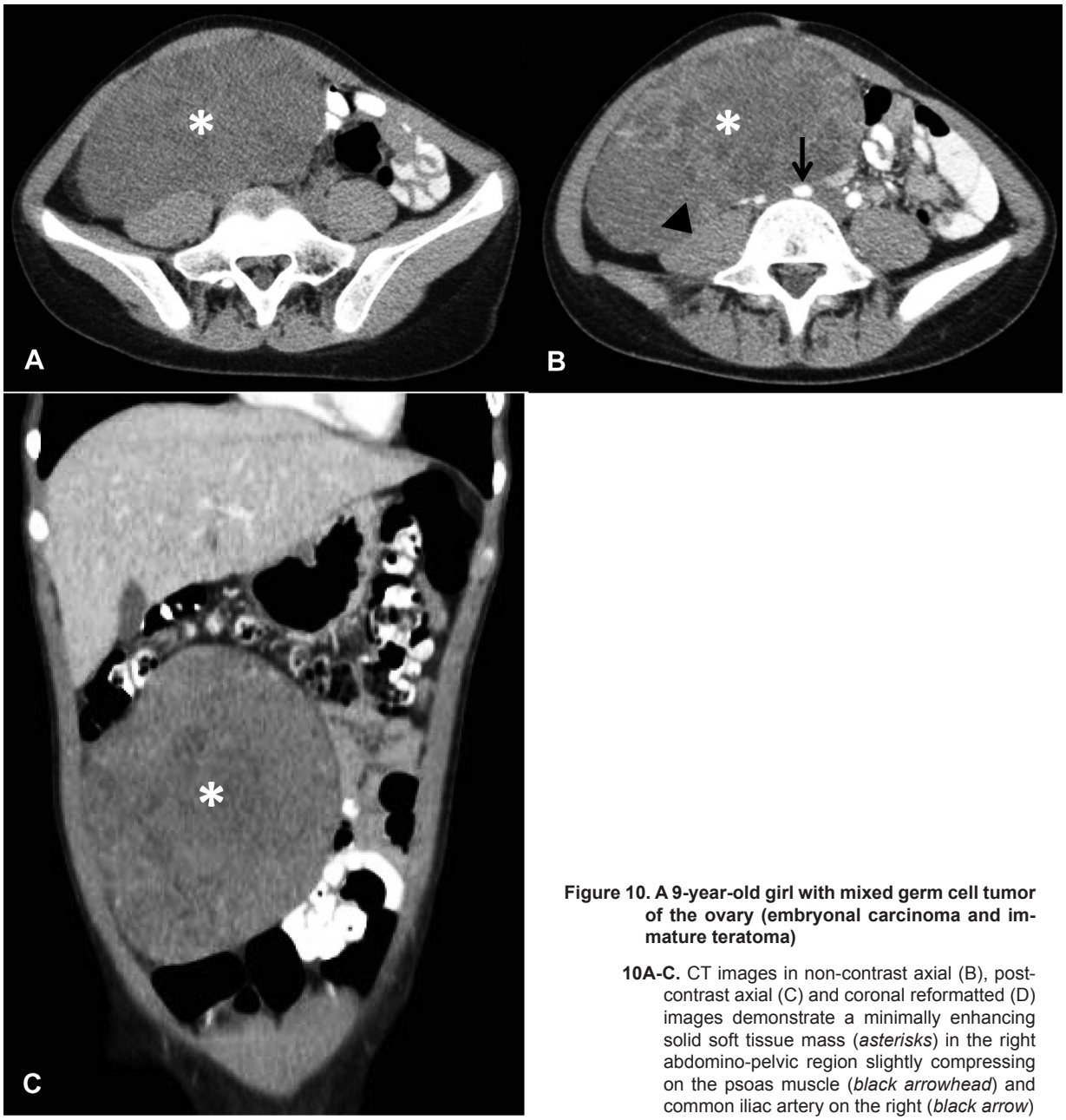

Figure 10. A 9-year-old girl with mixed germ cell tumor of the ovary (embryonal carcinoma and immature teratoma)

10A-C. CT images in non-contrast axial (B), post-contrast axial (C) and coronal reformatted (D) images demonstrate a minimally enhancing solid soft tissue mass (*asterisks*) in the right abdomino-pelvic region slightly compressing on the psoas muscle (*black arrowhead*) and common iliac artery on the right (*black arrow*)

cifications or small cysts which may be due to necrosis and hemorrhage. Spread to the pelvic and retroperitoneal lymph nodes is more frequent than intraperitoneal seeding.[30]

Malignant germ cell tumors metastasize to the lungs, liver, and peritoneum.

CONCLUSION

Ultrasound remains the primary screening tool for patients suspected to have an abdominal mass, as plain radiography has a very limited role. Computed Tomography and Magnetic Resonance Imaging are done for the diagnosis, staging, pre-operative management, follow-up and monitoring. Although abdominal tumors have similarities in their appearance, familiarity with the imaging characteristics is essential for radiologists to provide guidance for the clinicians.

REFERENCES

1. Chung EM, *et al*. Pediatric liver masses: radiologic pathologic correlation part 2 malignant lesions. Radiographics 2011; 31: 483-507.
2. Dubois J, LoweL. Neoplasia. Caffey's Pediatric Diagnostic Imaging. Saunders, 2013.
3. Lonergan GJ, Martinez-Leon M, *et al*. Nephrogenic rests, nephroblastomatosis and associated lesions of the kidney. Radiographics 1998; 18: 947-968.
4. Bates DG, FeinsteinK. Renal Neoplasms. Caffey's Pediatric Diagnostic Imaging. Saunders, 2013.
5. Kaste SC, McCarville B. Imaging Pediatric Abdominal Tumors. Semin Roentgenol2008; 43(1): 50-59.
6. Lowe LH, Isuani BH, HellerR. Pediatric renal masses: wilm's tumor and beyond. Radiographics 2000; 20: 1585-1603.
7. PapaiouannouG, McHughK. Neuroblastoma in childhood:review and radiological findings. Cancer Imaging 2005; 5: 116-127.
8. Elsayes KM, Mukundan G, NarraVR, *et al*. Adrenal masses: MR imaging features with pathologic correlation. Radiographics2004; 24: S73-S86.
9. Lowe G, Dliwayo H, LomasDJ. Adrenal neoplasms. Clinical Radiology 2012; 67 (10): 988-1000.
10. Moran DE. Periorbital ecchymosis ('racoon eyes') as the presenting feature of neuroblastoma. Pediatr Radiol 2010; 40: 1710.
11. Stanescu L, ParisiMT. 'Racoon eyes' revisited. Pediatr Radiol 2010; 40: S170.
12. Gu WZ, Zou CC, ZhaoZY. Childhood pancreatoblatoma: clinical features and immunohistochemistry analysis. Cancer letters 2008; 264: 119-126.
13. Cavallini A, Falconi M, *et al*. Pancreatoblastoma in adults: a review of literature. Pancreatology2009: 9: 73-80.
14. Nijs E, Callahan MJ, TaylorGA. Disorders of the pediatric pancreas: imaging features. Pediatr Radiol 2005; 35: 358-373.
15. Shah S, Mortele KJ. Uncommon solid pancreatic neoplasms: ultrasound, computed tomography and magnetic resonance imaging. Seminars in ultrasound, CT and MR2007; 28: 357-370.
16. Wang Y, Miller FH, ChenZE. Diffusion -weighted MR imaging of solid and cystic lesions of the pancreas. Radiographics2011; 31: E47-E65.
17. Roebuck DJ, Yuen MK, WongYC, *et al*. Imaging features of pancreatoblastoma. Pediatr Radiol2001; 31(7): 501-506.
18. Yang X. Imaging findings of pancreatoblastoma in 4 children including a case of ectopic pancreatoblastoma. Pediatr Radiol 2010; 40: 1609-1614.
19. Peddu P, Quaglia A, KanePA. Role of imaging in the management of pancreatic mass. Critical reviews in oncology / hematology2009; 70: 12-23.
20. Gupta AK, Mitra DK, Berry M, *et al*. Sonography and CT of pancreatoblastoma in children.AJR2000; 174: 1639-1641.
21. Lumkin B, Anderson MW, *et al*.CT, MRI, and Color Doppler Ultrasoundcorrelation of pancreatoblastoma: a case report. Pediatr Radiol 1993; 23(1): 61-62.
22. Toma P, *et al*. Multimodality Imaging of Hodgkin Disease and Non-Hodgkin Lymphoma in Children. Radiographics 2007; 27: 1335-1354.
23. globocan.iarc.fr/Pages/online.aspx
24. Bakhshi, *et al*. Pediatric nonlymphoblastic non-hodgkin lymphoma: baseline, interim, and postreatment PET/CT versus contrast-enhanced CT for evaluation - a prospective study. Radiology 2012; 262: 956-968.
25. Van Rijn RR, *et al*. Imaging findings in noncraniofacial childhood rhabdomysarcoma. Pediatr Radiol 2008; 38: 617-634.
26. Shresta A, *et al*. Early life factors and risk of childhood rhabdomyosarcoma. Frontiers in public health 2013; 1: 1-8.
27. Diaconcescu S, *et al*. Childhood rhabdomyosarcoma. Anatomo-Clinical and therapeutic study on 25 cases. Surgical Implications. Rom J Morphol Embryol2013; 54 (3): 531-537.
28. Leung RS, *et al*. Embryonal rhabdomyosarcoma of the omentum: two cases. Pediatr Radiol2009; 39: 865-868.
29. Geoffray A, Couanet D, *et al*. Ultrasonography and CT for diagnosis and follow-up of pelvic rhabdomyosarcomas in children. Pediatr Radiol1987; 17(2): 132-136.
30. Epelman M, *et al*.Imaging of pediatric ovarian neoplasms. Pediatr Radiol 2011; 41: 1085-1099.
31. Zhang M, Jiang W, *et al*. Ovarian masses in children and adolescents - an analysis of 521 clinical cases. J Pediatr Adolesc Gynecol2014; 27(3): e73-e77.